CHAPTER IV
RESULTS AND DISCUSSION

Chapter IV presents the complete experimental results, including the structural characterization of the synthesized β–Zn_4Sb_3 powders and the thermoelectric properties of sintered β–Zn_4Sb_3 pellets. This chapter also includes the analysis and evaluation of monolithic β–Zn_4Sb_3/ZnO TEG modules. he results are presented according to scientific hypotheses and specific theories. This chapter is divided into five sections: X–ray diffraction, X–ray absorption, thermoelectric properties, module analysis and evaluation, respectively.

4.1 X–ray diffraction

According to the synthesis of β–Zn_4Sb_3 powders, the process synthesis of β–Zn_4Sb_3 powders were investigated using comparative X–ray diffraction (XRD) pattern of the synthesized β–Zn_4Sb_3 powders, along with calculated XRD pattern of β–Zn_4Sb_3 of Mayer's model. Initially, the optimal calcination temperature for the synthesis of β–Zn_4Sb_3 powders without excess Zn powder was determined by comparing temperatures of non-calcined, 300 °C, 400 °C and 500 °C, and held for 3 hours. The experimental results indicate that the optimal calcination temperature for synthesis β–Zn_4Sb_3 powders without excessing of Zn powder is condition of calcination temperature at 400 °C, as it produced essential 3 peaks around $2\boldsymbol{\theta}$ ~ 25° in the XRD pattern of β–Zn_4Sb_3 materials. Comparative XRD patterns of the synthesized β–Zn_4Sb_3 powders without excessing of Zn powder for calcination temperature of non–calcined, 300 °C, 400 °C and 500 °C are shown in Figure 49.

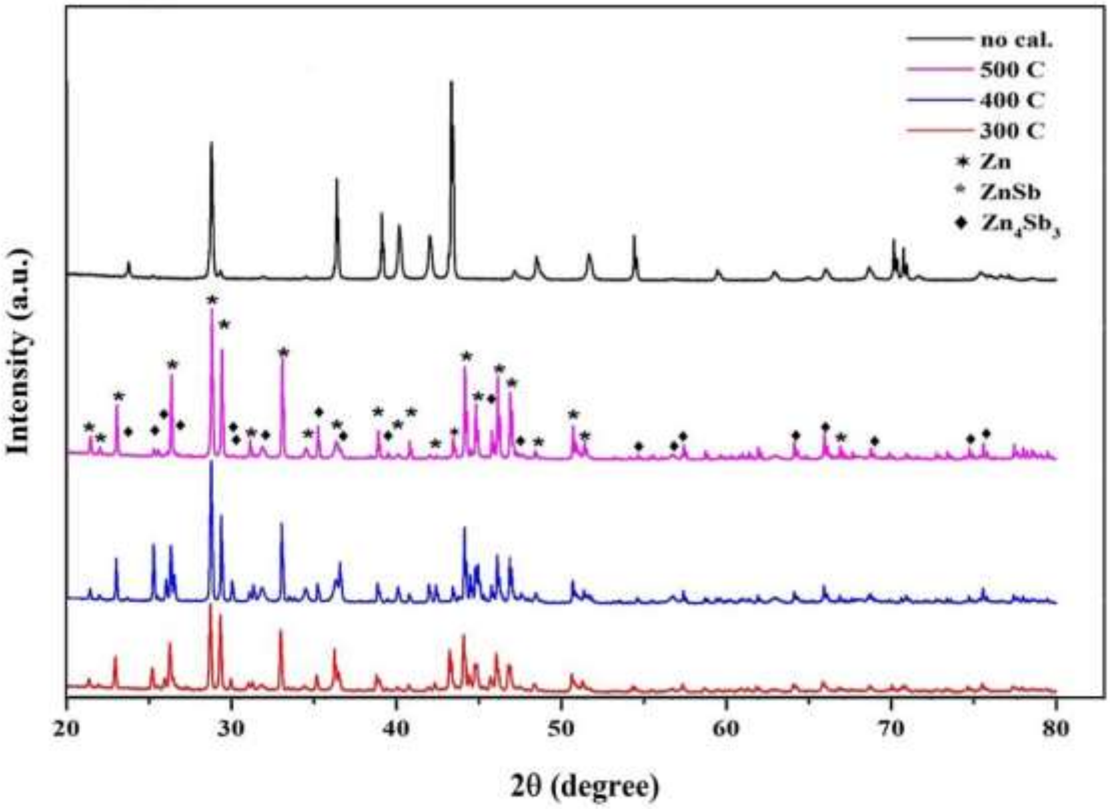

Figure 49 X–ray diffraction patterns of the synthesized β–Zn_4Sb_3 powders under conditions of calcination temperature non–calcined, 300 °C, 400 °C and 500 °C without excess of Zn.

The optimal calcination temperature for synthesizing β–Zn_4Sb_3 powders without excessing of Zn powder is 400 °C. To investigate the effects of varying amounts of excess Zn, different conditions were tested by adding 0, 5, 10, 15 and 20 at.% Zn to the premixed powders. The XRD pattern results indicate that the optimal amount of excess Zn powder is 10 at.% because the XRD pattern of the synthesized β–Zn_4Sb_3 powders with this addition closely resembles of Mayer's model. The comparison XRD pattern of the synthesized β–Zn_4Sb_3 powders under varying excessed Zn conditions at a calcination temperature of 400 °C for 3 hours are shown in Figure 50.

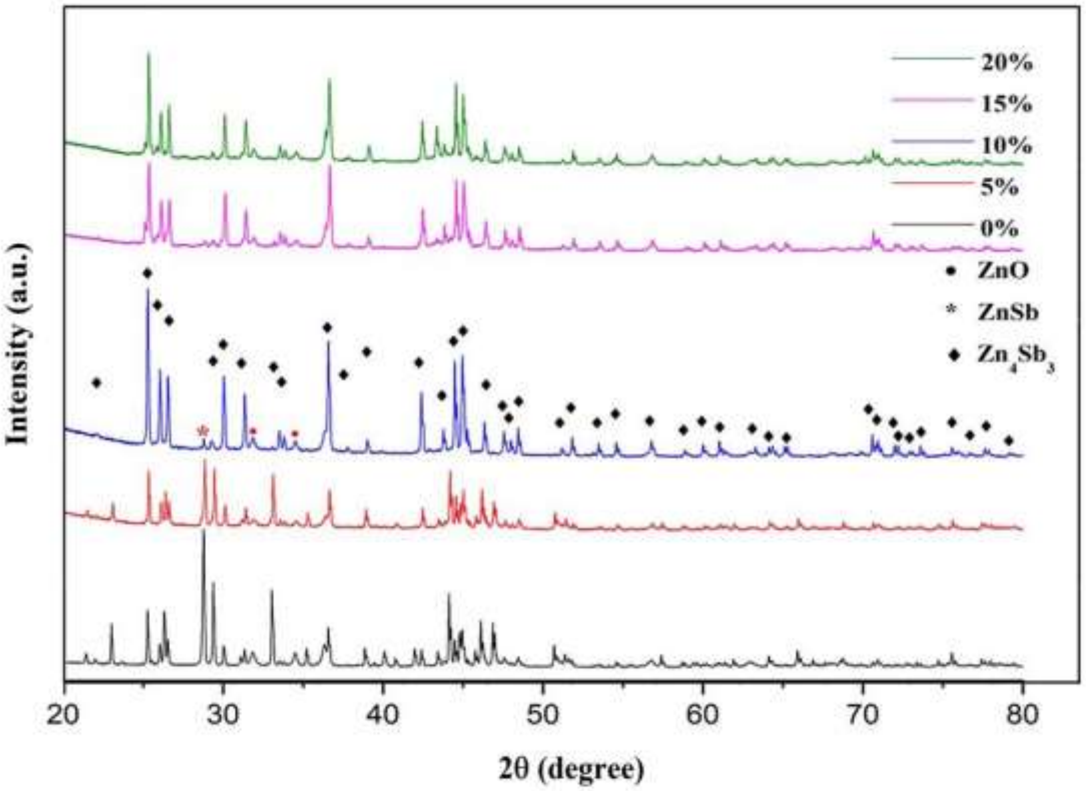

Figure 50 The comparison XRD pattern of the synthesized β–Zn_4Sb_3 powders under varying excessed Zn condition via calcination temperature 400 °C and held for 3 hours.

The optimal conditions for synthesizing β–Zn_4Sb_3 powders is usage excess of 10 at.% Zn powder and calcination at 400 °C for 3 hours. The calcination holding time was then for 1, 3 and 5 hours. The XRD pattern results show that calcination holding time for 3 hours produces the best XRD pattern for the synthesized β–Zn4Sb3 powders, closely matching XRD pattern of β–Zn_4Sb_3 of Mayer’s model and outperforming other conditions. Although the XRD pattern under calcination holding time for 3 hours resembles under calcination holding time for 3 hours. Indeed, the XRD pattern of the synthesized β–Zn_4Sb powders under calcination holding time for 3 hours has clearer peaks and higher intensity. The comparison XRD pattern of the synthesized β–Zn_4Sb_3 powders under varying holding time, using excess Zn of 10 at.% and calcination temperature of 400 °C are shown in Figure 51.

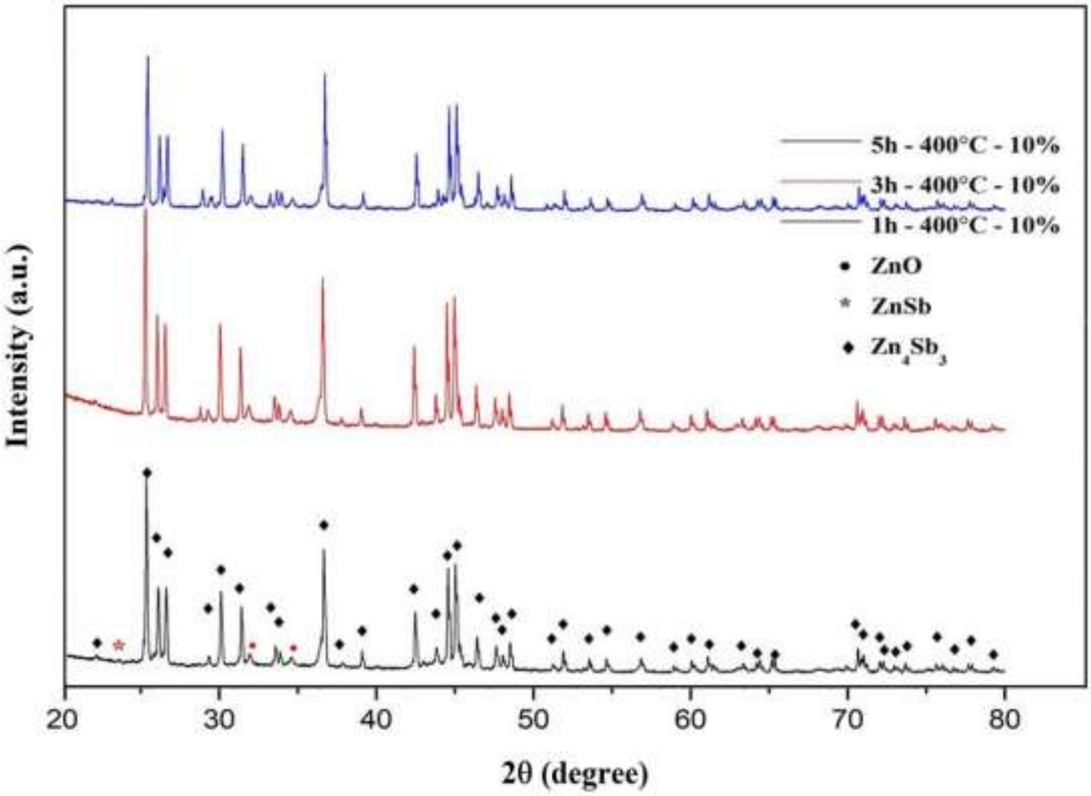

Figure 51 XRD pattern of varying holding time via excessing Zn of 10 at.% Zn and calcination temperature 400 °C.

Currently, the optimal conditions for synthesizing β–Zn_4Sb_3 powders is excess 10 at.% Zn and calcination temperature of 400 °C for 3 hours. To further refine these conditions, calcination temperature 350 °C, 400 °C and 450 °C were investigated. The XRD pattern results indicate that a calcination temperature condition of 450 °C yields a better XRD pattern for β–Zn_4Sb_3 materials better compared to 400 °C, due to reduced impurity phases of ZnSb, Zn and Sb. The comparison of XRD pattern for the synthesized β–Zn_4Sb_3 powders under conditions of calcination temperature at 350 °C, 400 °C and 450 °C is shown in Figure 52.

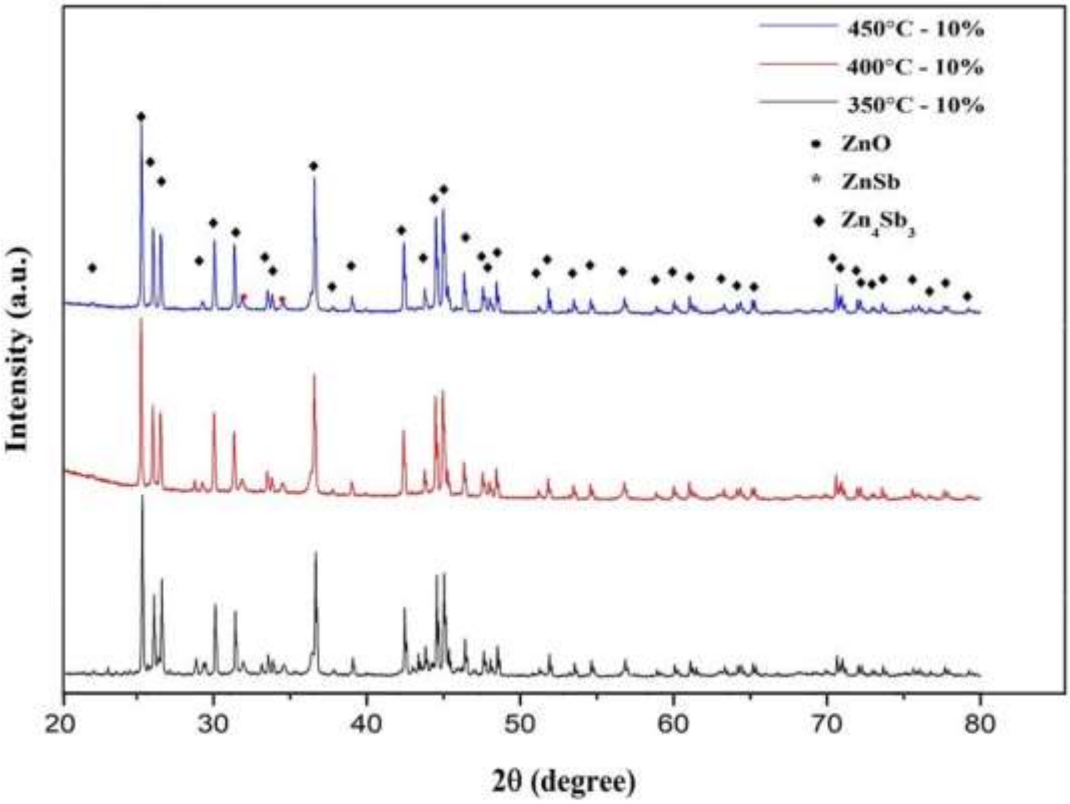

Figure 52 The comparison XRD pattern of the synthesized β–Zn_4Sb_3 powders under varying calcination temperature at 350 °C, 400 °C and 450 °C via adding 10 at.% Zn and calcination holding time for 3 hour.

Under the current conditions, the optimal synthesis for β–Zn_4Sb_3 powders involves using excess Zn powders 10 at.% and calculating at 450 °C for 3 hours. To further refine, conditions of excess Zn powders as 10, 11, 12, 13, 14 at.% were subjected to the same calcination process. As depicted in Figure 53, the XRD diffraction pattern of the synthesized β–Zn_4Sb_3 powders under 12 at.% Zn rich at calcination temperature at 450 °C for 3 hours produced the best results, with minimal impurity phases of ZnSb, Zn and Sb.

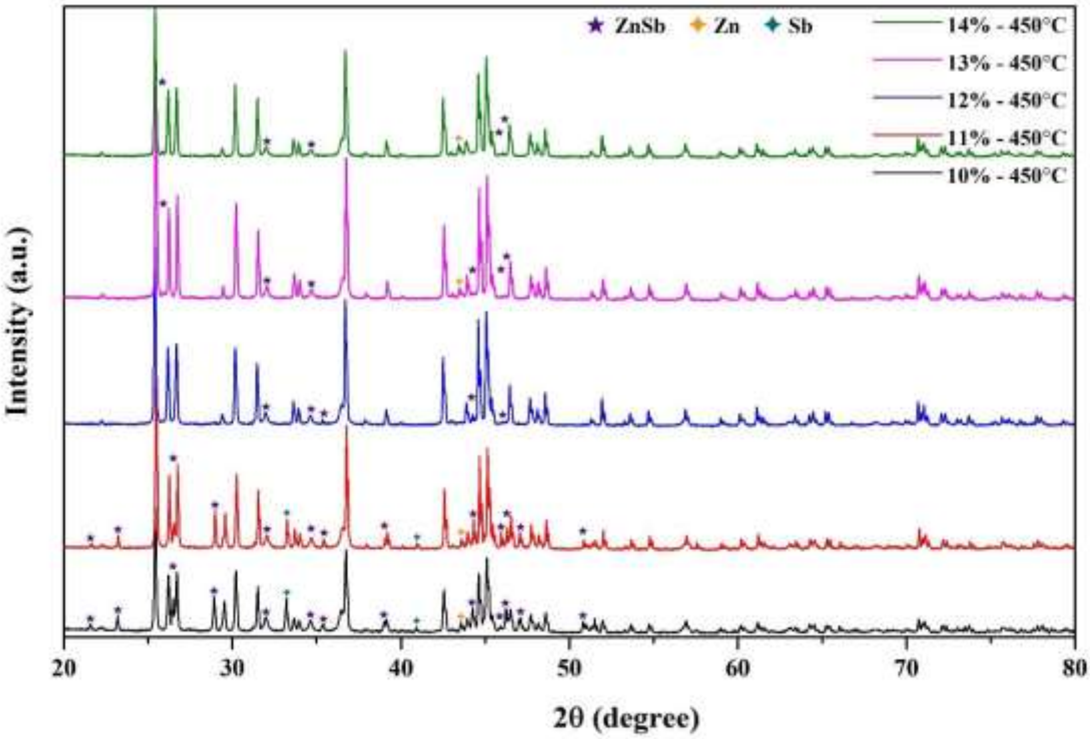

Figure 53 Comparison XRD pattern of the synthesized β–Zn_4Sb_3 powders under excessing Zn for 10, 11, 12, 13 and 14 at.% Zn and calcination at 450 °C for 3 hours.

Additionally, calcination temperature of 400 °C and 425 °C were investigated with excess Zn powders as 10, 11, 12, 13, 14 at.%. As shown in Figure 54 and Figure 55, the XRD diffraction pattern of the synthesized β–Zn_4Sb_3 powders under calcination temperature at 400 °C and 425 °C with excess Zn powders as 10, 11, 12, 13, 14 at.% Zn, indicate that the best results for both 400 °C and 425 °C were obtained with excess Zn powders 13 at.%, as depict in Figure 54 and Figure 55. Finally, Figure 56 compares the XRD patterns for the best synthesis conditions: 400 °C with 13 at.% Zn, 425 °C with 13 at.% Zn and 450 °C with 12 at.% Zn, all with a holding time of 3 hours. Among these, the optimal condition for synthesizing β–Zn_4Sb_3 powders is excess Zn powders 12 at.% under calcination temperature 450 °C for 3 hours, as it results in the least amount of impurity phases

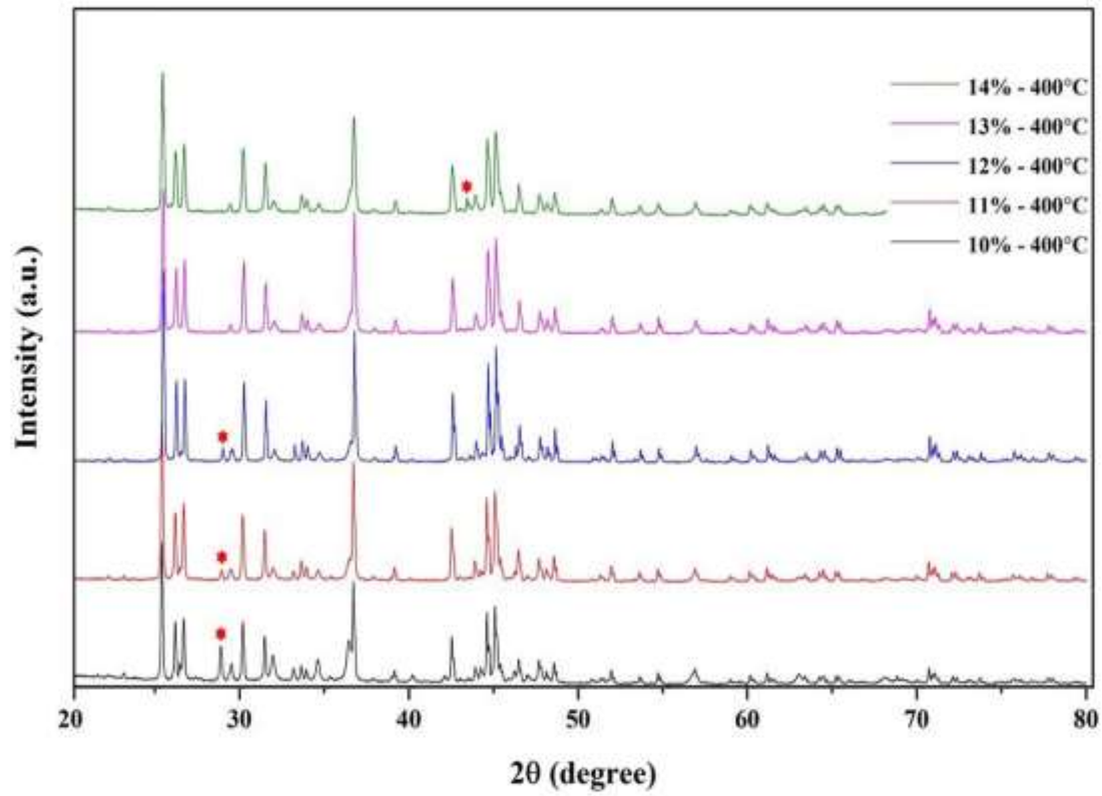

Figure 54 Comparison XRD pattern of the synthesized β–Zn_4Sb_3 powders under excessing Zn for 10, 11, 12, 13 and 14 at.% Zn and calcination at 400 °C for 3 hours.

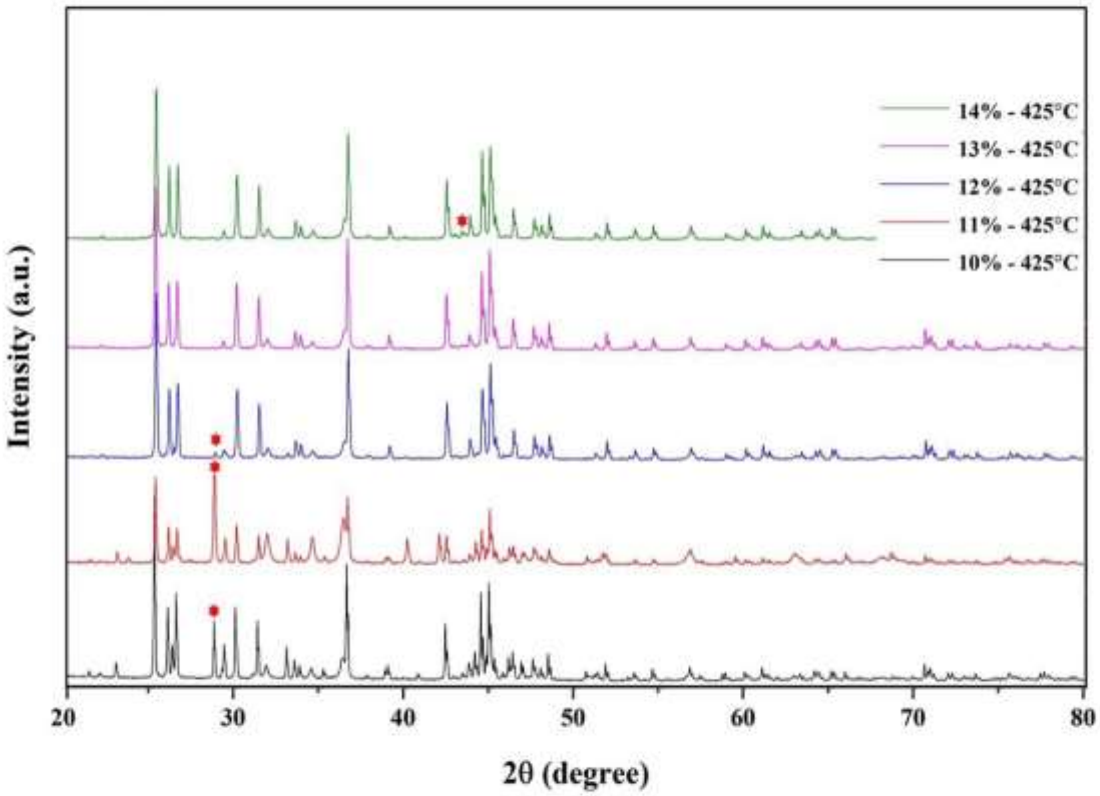

Figure 55 Comparison XRD pattern of the synthesized β–Zn_4Sb_3 powders under excessing Zn for 10, 11, 12, 13 and 14 at.% Zn and calcination at 425 °C for 3 hours.

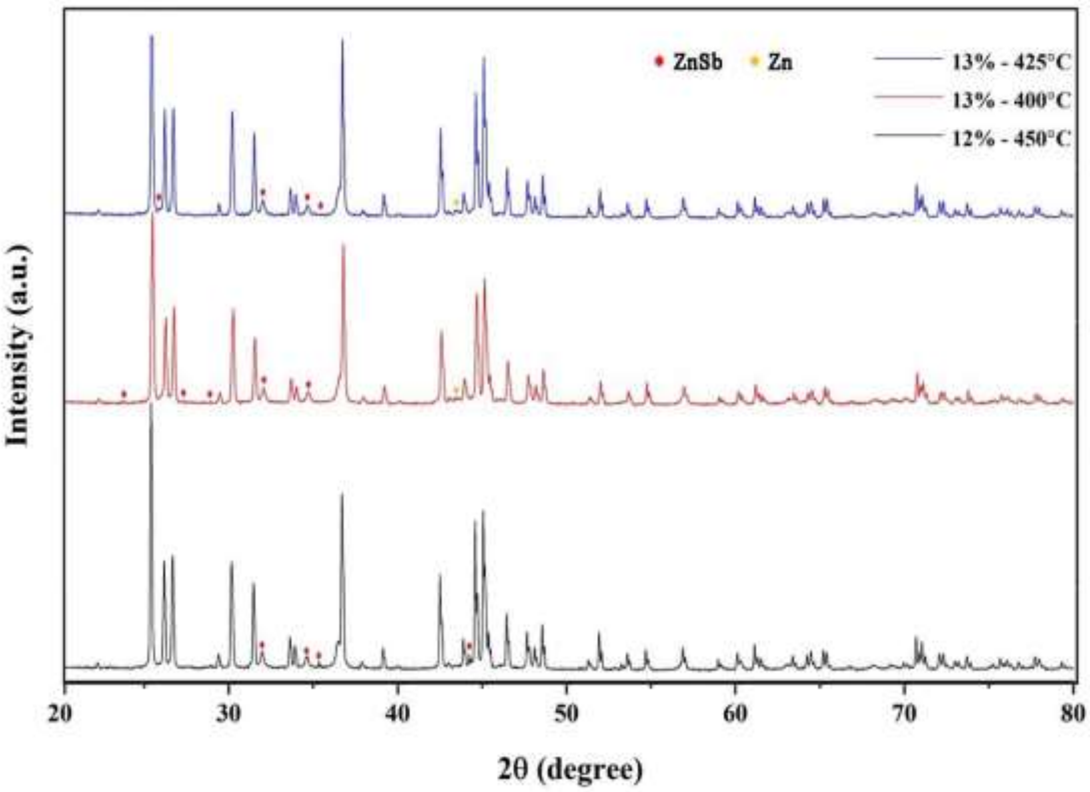

Figure 56 Comparison of the synthesis series of excessing Zn for 10, 11, 12, 13, 14 and 15 at.% Zn and calcination at 400 °C, 425 °C, 450 °C for 3 hours.

4.2 X–ray absorption spectroscopy

The purest β–Zn_4Sb_3, synthesized with excessing 12 at.% Zn rich at a calcination temperature of 450 °C for 3 hours, were investigated using x–rays absorption near–edge structure (XANES) spectra at the Zn K–edge and Sb L–edges. This analysis was conducted at SUT–NANOTEC–SLRI XAS beamline (BL 5.2) using synchrotron. The exciting core electrons as oxidation states of Zn atoms in the synthesized β–Zn_4Sb_3 powder were measured at level K (Zn K–edge) across energy range 9,550–9800 eV, as shown in Figure 57. The normalized XANES spectrum of the Zn K–edge reveals a rising energy edge range of 9,640–9,667, with the main absorption edge at 9,659 eV. Then, the derivation of normalized XANES spectrum of the Zn K–edge of the synthesized β–Zn_4Sb_3 powders further confirms the main absorption edge at 9,659 eV, as expressed in Figure 58.

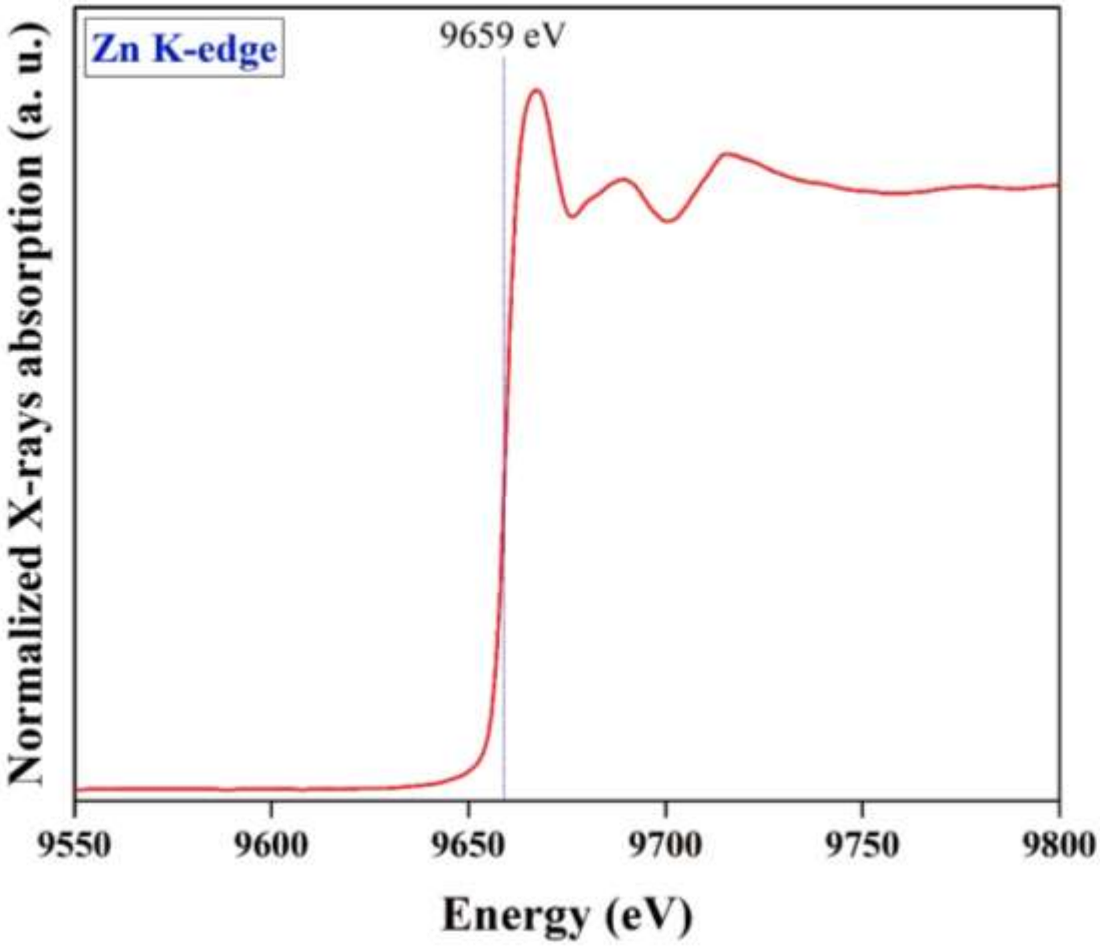

Figure 57 Normalized XANES of Zn K–edge of the high pure synthesized β–Zn_4Sb_3 powder.

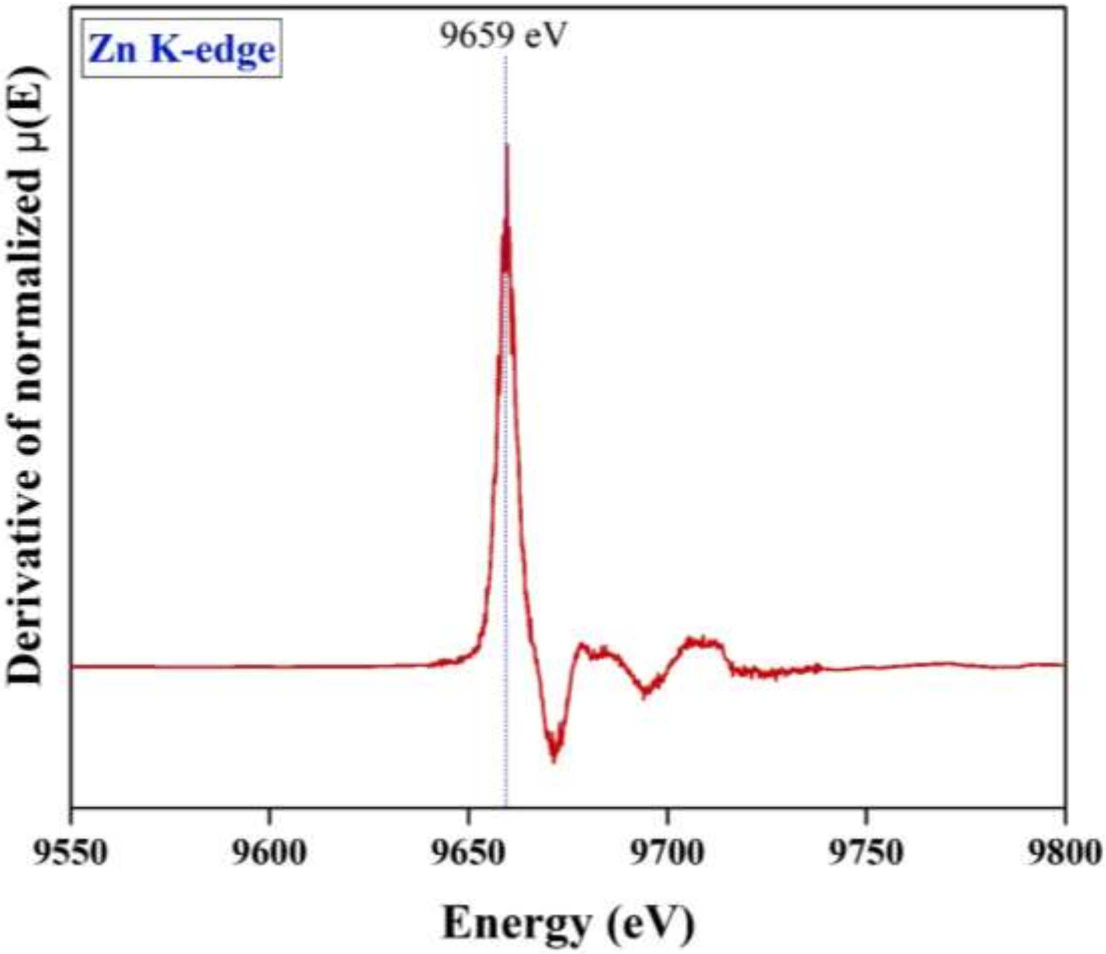

Figure 58 Derivative normalized XANES of Zn K–edge of the high pure synthesized β–Zn_4Sb_3 powder.

The exciting core electrons as oxidation states of Sb atoms in the synthesized β–Zn_4Sb_3 powders were measured at level L (Sb L–edges) across energy range 4,000–4,750 eV, as shown in Figure 59. The normalized XANES spectrum for the Sb L3, L2 and L1–edge reveal rising energy edges range of 4,100–4,150 eV, 4,377–4,397 eV and 4,690–4,700 eV, with the main absorption edges at 4,132 eV, 4,380 eV and 4,698 eV, respectively. Then, the derivation of normalized XANES spectrum for the Sb L3, L2 and L1–edge of the synthesized β–Zn_4Sb_3 powders further confirms these main absorption, as shown in Figure 60.

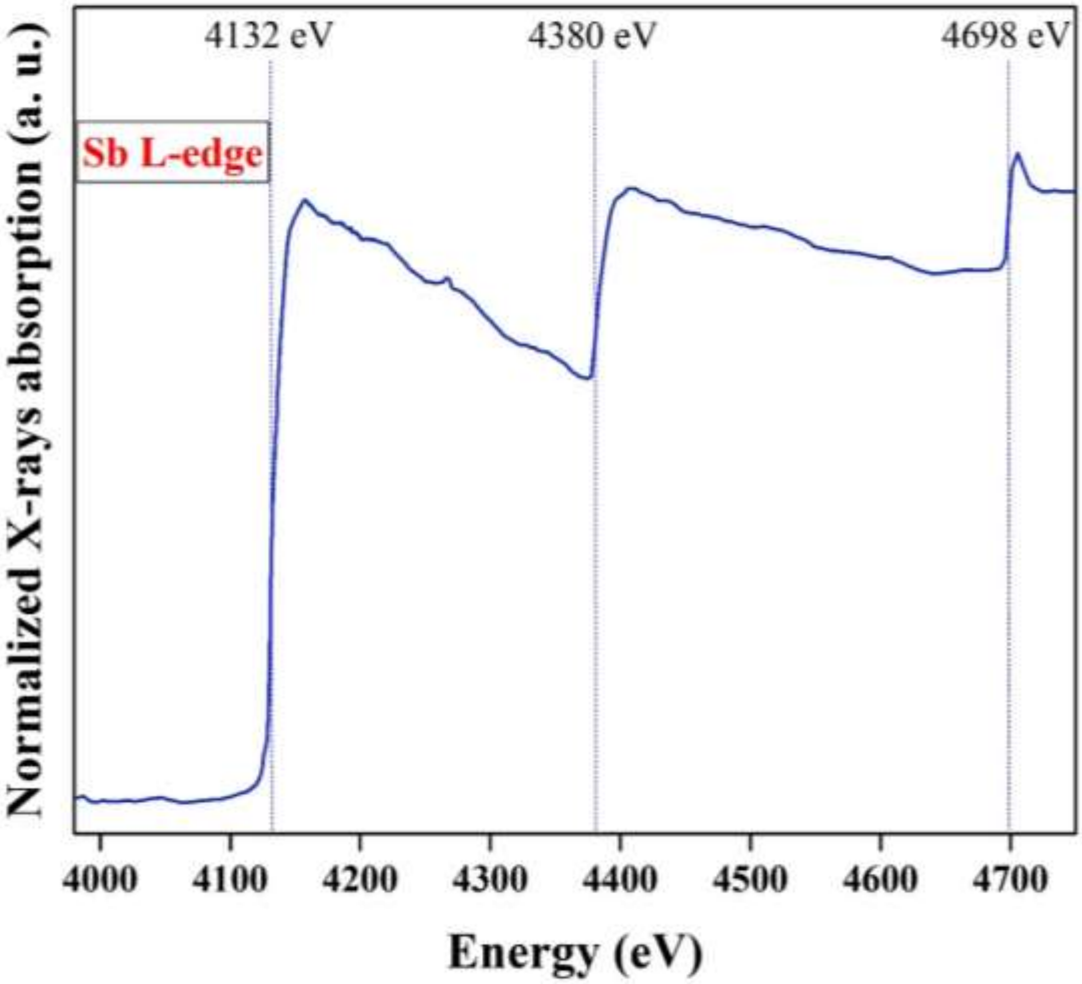

Figure 59 Normalized XANES of Sb L3, L2 and L1–edge of the high pure synthesized β–Zn_4Sb_3 powder.

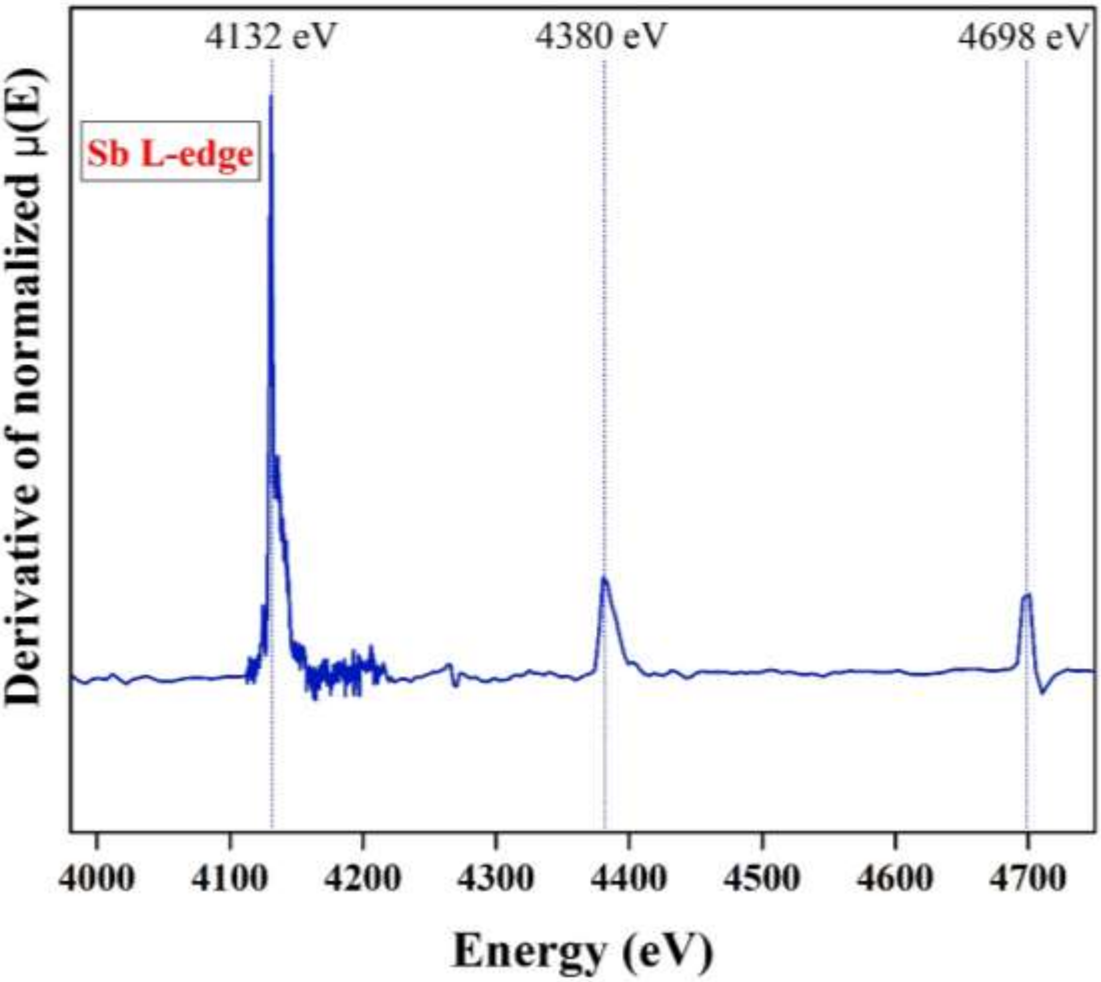

Figure 60 Derivative normalized XANES of Sb L3, L2 and L1–edge of the high pure synthesized β–Zn_4Sb_3 powder.

Originally, β–Zn_4Sb_3 is an alloy material with characteristic ionization energies of exciting core electrons as oxidation states of Zn^0 and Sb^0. Based on the experimental results from the normalized XANES and derivative normalized XANES spectra of the Zn K–edge and Sb L–edges for the high pure synthesized β–Zn_4Sb_3 powders, it is confirmed that the ionization energy of exciting core electrons as oxidation state correspond to the Zn^0 and Sb^0 oxidation states. This finding aligns with the absorption edge database of the Hephaestus program (Ravel and Newville, 2005) and further confirms that the synthesized β–Zn_4Sb_3 powders is devoid of existing ionic bonding and oxides.

4.3 Thermoelectric properties

The high pure synthesized β–Zn_4Sb_3 powder were used to fabricate the sintered β–Zn_4Sb_3 pellets. The thermoelectric properties of these sintered pellets, including Seebeck coefficient, electrical resistivity and electrical power factor, were measured using Linseis LSR–3 equipment. The Seebeck coefficient of the sintered β–Zn_4Sb_3 pellets, under produced under pressing pressure of 700 MPa and sintering temperature at 500 °C, 525 °C and 550 °C were measured across varying operating temperature. A comparison of the Seebeck coefficient is shown in Figure 61. The Seebeck coefficient of all sample increased with rising operating temperature up to 300 °C, after which the Seebeck coefficient continued decreased. The experimental results are consistent with literature reports (Lee and Lin, 2018; Kunioka *et al.*, 2018). The Seebeck coefficients of the sintered β–Zn_4Sb_3 pellets at sintering temperatures of 500 °C, 525 °C and 550 °C are 255 μV/°C, 216 μV/°C and 191 μV/°C, respectively. The positive Seebeck coefficient values of the sintered β–Zn_4Sb_3 pellets confirms that the sintered pellets are p–type thermoelectric materials. The sintered β–Zn_4Sb_3 pellets under condition of pressing pressure 700 MPa and sintering temperature at 500 °C showed the highest Seebeck coefficient at an operating temperature of 320 °C, as shown in Figure 61.

In addition to the Seebeck coefficient, the electrical resistivity was also measured. As depicted in Figure 62, the electrical resistivity of all sintered β–Zn_4Sb_3 pellets samples gradually decreased with increasing operating temperature until reaching 200 °C.

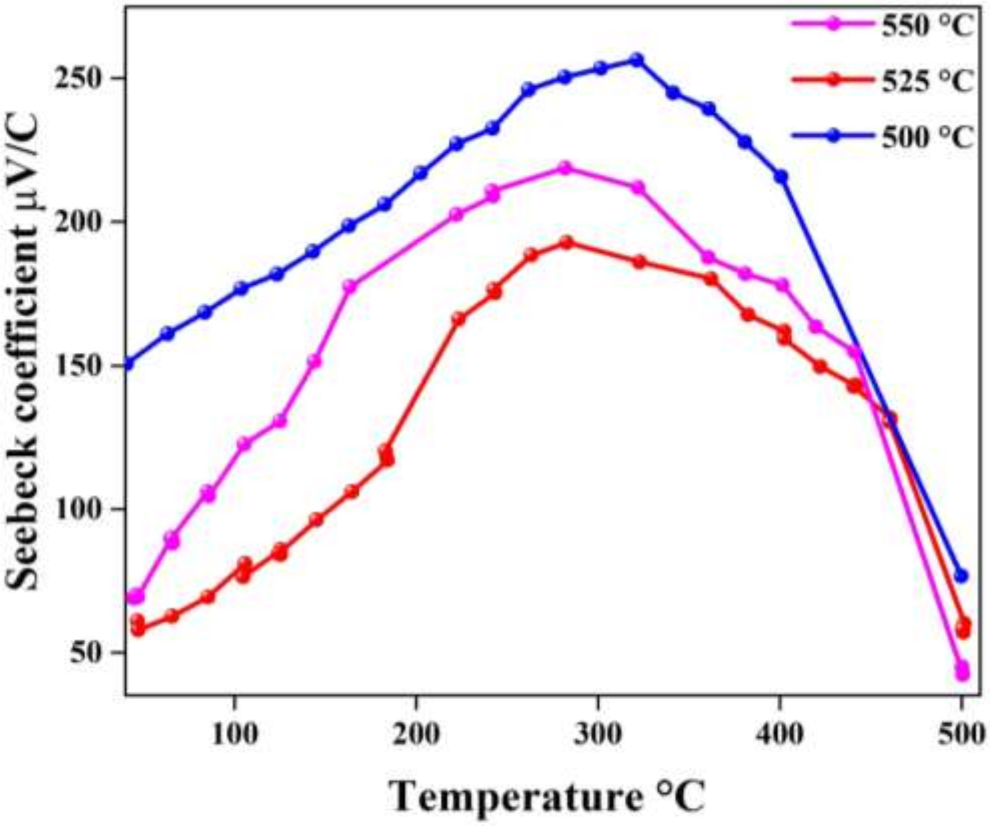

Figure 61 Seebeck coefficient of the sintered β–Zn_4Sb_3 pellets versus varying temperature.

The electrical resistivity of all samples remains constant across the operating temperature range of 200–480 °C. The electrical resistivity of the sintered β–Zn_4Sb_3 pellets within this temperature range is approximately $1.25\text{x}10^{-6}$ Ω.m for the sample sintered at 500 °C, $1.60\text{x}10^{-6}$ Ω.m for the sample sintered at 500 °C, and 1.90 $\text{x}10^{-6}$ Ω.m for the sample sintered at 500 °C. Although the electrical resistivity curves of all samples are similar, the pellet sintered under a condition of pressing pressure of 700 MPa with sintering temperature of 500 °C stands out, exhibiting the lowest electrical resistivity and thus the highest electrical conductivity. High electrical conductivity positively impacts the figure of merit, as indicated by Equation (96), which reflects superior thermoelectric properties.

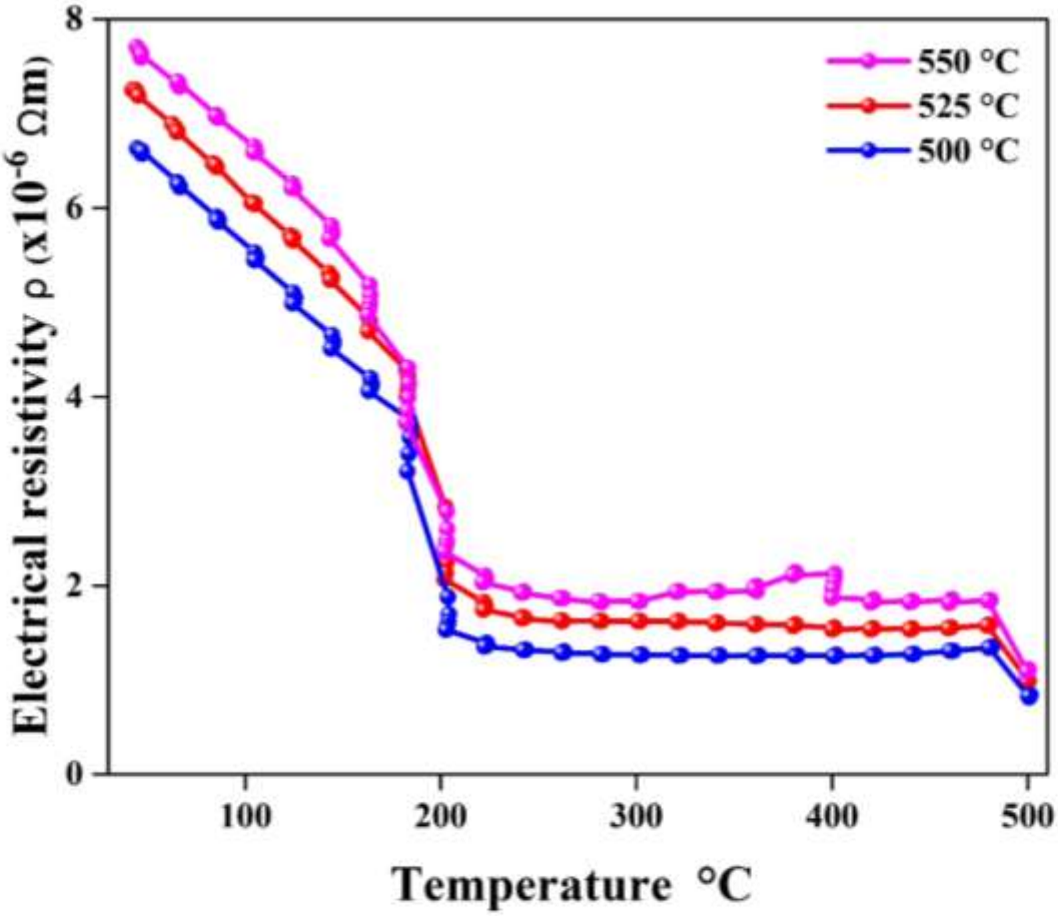

Figure 62 Electrical resistivity of the sintered β–Zn_4Sb_3 pellets versus varying temperature.

The performance of thermoelectric materials is evaluated by electrical power factor. The electrical power factor of the sintered β–Zn_4Sb_3 pellets was measured across varying operating temperature. As shown in Figure 63, the electrical power factor exhibits significant fluctuations, which may be attributed to the inherent properties of the sintered β–Zn_4Sb_3 pellets and potential issues with the measurement equipment. Despite this, the results suggest that the optimal operating temperature for all sintered β–Zn_4Sb_3 pellets is approximately across temperature range 200–300 °C.

Consequently, a monolithic multi–stack β–Zn_4Sb_3/ZnO TEG module were fabricated under condition of pressing pressure of 700 MPa and sintering temperature at 500 °C. This module was tested for performance at operating temperature at 200 °C and 300 °C, corresponding to the highest Seebeck coefficient of 255 μV/°C at 320 °C and the optimal operating temperature range (high power factor) of 200–300 °C.

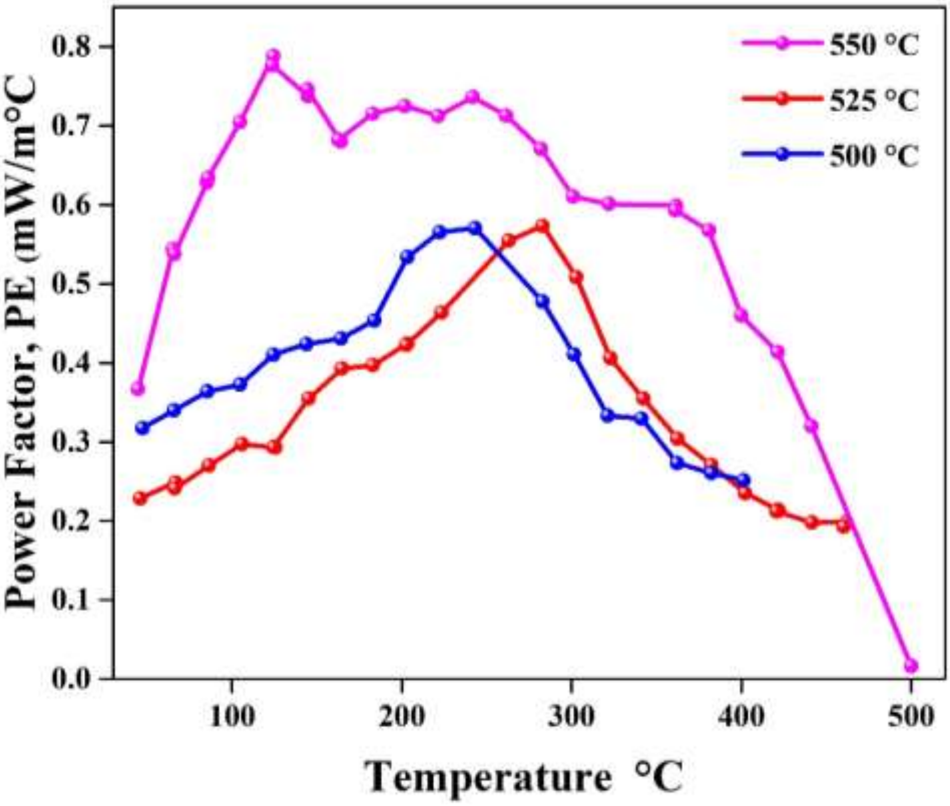

Figure 63 Electrical power factor of the sintered β–Zn_4Sb_3 pellets versus varying temperature.

4.4 Module analysis and evaluation

The performance of test cells of monolithic β–Zn_4Sb_3/ZnO TEG modules and monolithic multi–stack β–Zn_4Sb_3/ZnO TEG modules was evaluated using a custom-built heating/cooling system with IV measurement capabilities. Initially, the test cells of the monolithic β–Zn_4Sb_3/ZnO TEG modules were assessed for IV characteristics and electrical power output curves. Based on the results, the monolithic multi–stack β–Zn_4Sb_3/ZnO TEG modules were fabricated under the condition of the test cells that expressed the best IV–characteristics and electrical power output curves. The test cells were investigated under different conditions, with varying weights of β–Zn_4Sb_3 powders : 0.2 g, 0.5 g, 1 g, 2 g and 4 g applied to each side of the β–Zn_4Sb_3 component (Figure 40). Open–circuit voltage (V_{op}) and short circuit current (I_{sc}) were measured, representing the maximum potential difference and current between the charge terminals of the modules, respectively. The V_{op} and I_{sc} measurements of the test cells under condition of weight 0.2 g, 0.5 g, 1 g, 2 g and 4 g were conducted under operating conditions with a hot side temperature (T_h) of 100 °C and gradient temperature (ΔT) of 50 °C, T_h=200 °C–ΔT=50 °C, T_h=200 °C –ΔT=100 °C, T_h=300 °C –ΔT=50 °C and T_h=300 °C –ΔT=100 °C. The V_{op} and I_{sc} results of all the test cells of monolithic β–Zn_4Sb_3/ZnO TEG modules under these conditions are presented in Table 6. The V_{op} and I_{sc} values showed an increase with rising hot side temperature and temperature gradient. The maximum V_{op} and I_{sc} values for the test cells under condition weight of 0.2 g, 0.5 g, 1.0 g, 2.0 g, 4.0 g are 23.1 mV, 38.1 mV, 45.4 mV, 39.5 mV 41.2 mV, and 8.81 mA, 16.71 mA, 19.87 mA, 16.25 mA, 11.26 mA, respectively at T_h=300 °C–ΔT=100 °C. Although the maximum V_{op} and I_{sc} for the test cells under condition weight of 0.5 g, 1.0 g, 2.0 g and 4.0 g were quite good, the test cells under condition of 1 g was the best, achieving the highest maximum electrical power output of 595 μW (Figure 65) and the highest V_{op} of 45.4 V at the operating hot side temperature of 300°C –ΔT=100 °C.

Table 6 List of open–circuit voltage (V_{op}) and short circuit current (I_{sc}) versus varying operating condition temperature of the test cells of monolithic couple β–Zn_4Sb_3/ZnO TEGs with condition of 0.5 g, 1.0 g, 2.0 g and 4.0 g.

Test cells conditions (g)	100°C, ΔT 50°C		200°C, ΔT 50°C		200°C, ΔT 100°C		300°C, ΔT 50°C		300°C, ΔT 100°C	
	V_{op} (mV)	I_{sc} (mA)	V_{op} (mV)	I_{sc} (mA)	V_{op} (mV)	I_{sc} (mA)	V_{op} (mV)	I_{sc} (mA)	V_{op} (mV)	I_{sc} (mA)
0.2	5.4	2.12	10.7	4.11	13.7	5.33	12.4	5.11	23.1	8.81
0.5	8.8	1.74	13.8	5.09	28.9	9.62	20.8	8.86	38.1	16.71
1	16.2	6.07	24.1	11.50	31.8	15.61	24.7	11.87	45.4	19.87
2	11.3	4.00	20.9	8.43	29.6	12.02	27.7	11.09	39.5	16.29
4	9.3	1.60	18.9	4.67	23.1	6.55	18.4	4.30	41.2	11.26

Therefore, test cells condition of 1.0 g was selected to applied in fabrication of the multi–stack β–Zn_4Sb_3/ZnO TEG modules. Moreover, the IV–curve and electrical power output curve of the test cells of monolithic β–Zn_4Sb_3/ZnO TEG module under condition of 1.0 g are shown in Figure 64 and Figure 65, respectively.

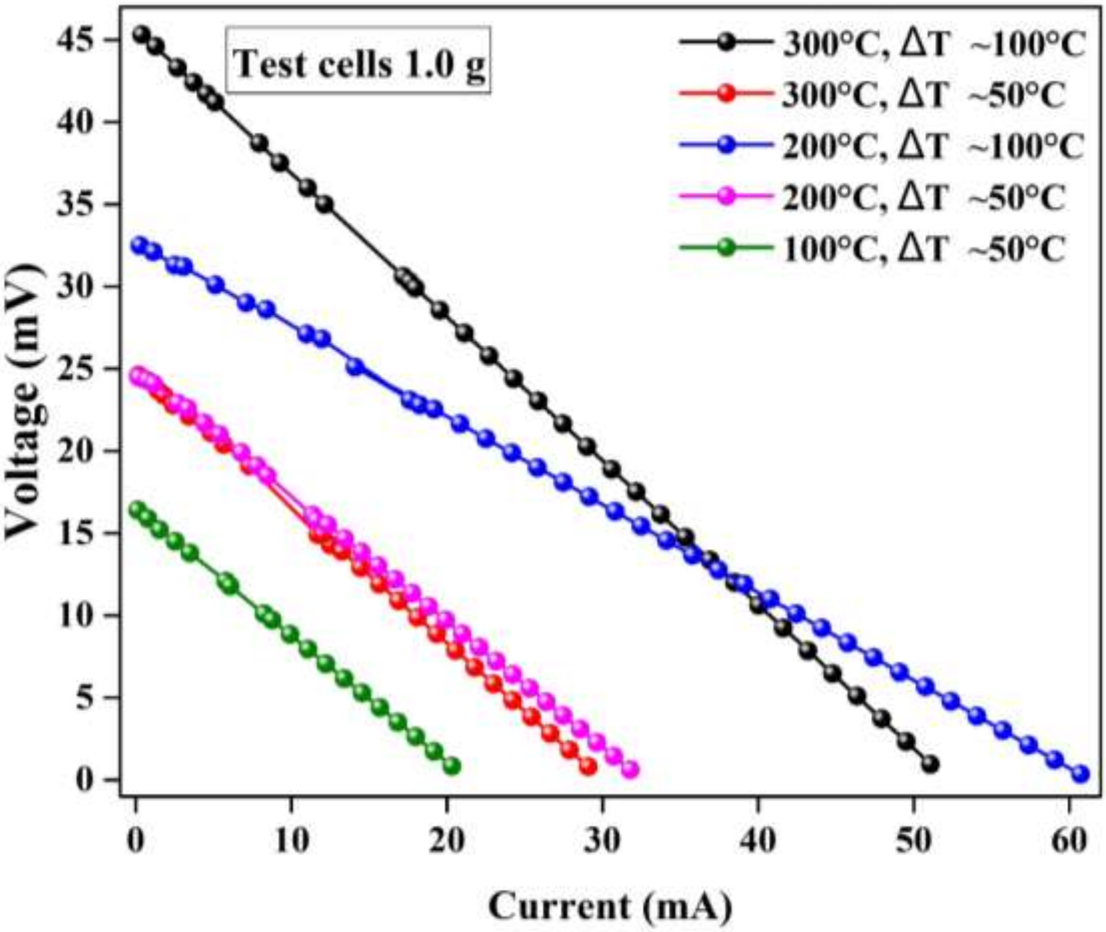

Figure 64 IV–curve of the test cells of monolithic β–Zn_4Sb_3/ZnO TEGs under condition of weight 1.0 g versus different operating T_h and ΔT.

The IV–curve of the test cells of monolithic β–Zn_4Sb_3/ZnO TEG module under condition weight of 1.0 g reveals a significant area under the curve at operating conditions of T_h=300 °C –ΔT=100 °C and T_h=200 °C –ΔT=100 °C. Moreover, the maximum power output of these test cells is approximately 595 µW at T_h=300 °C –ΔT=100 °C. A comparison of the maximum electrical power output (P_{out}) under operating temperatures is presented in Table 7.

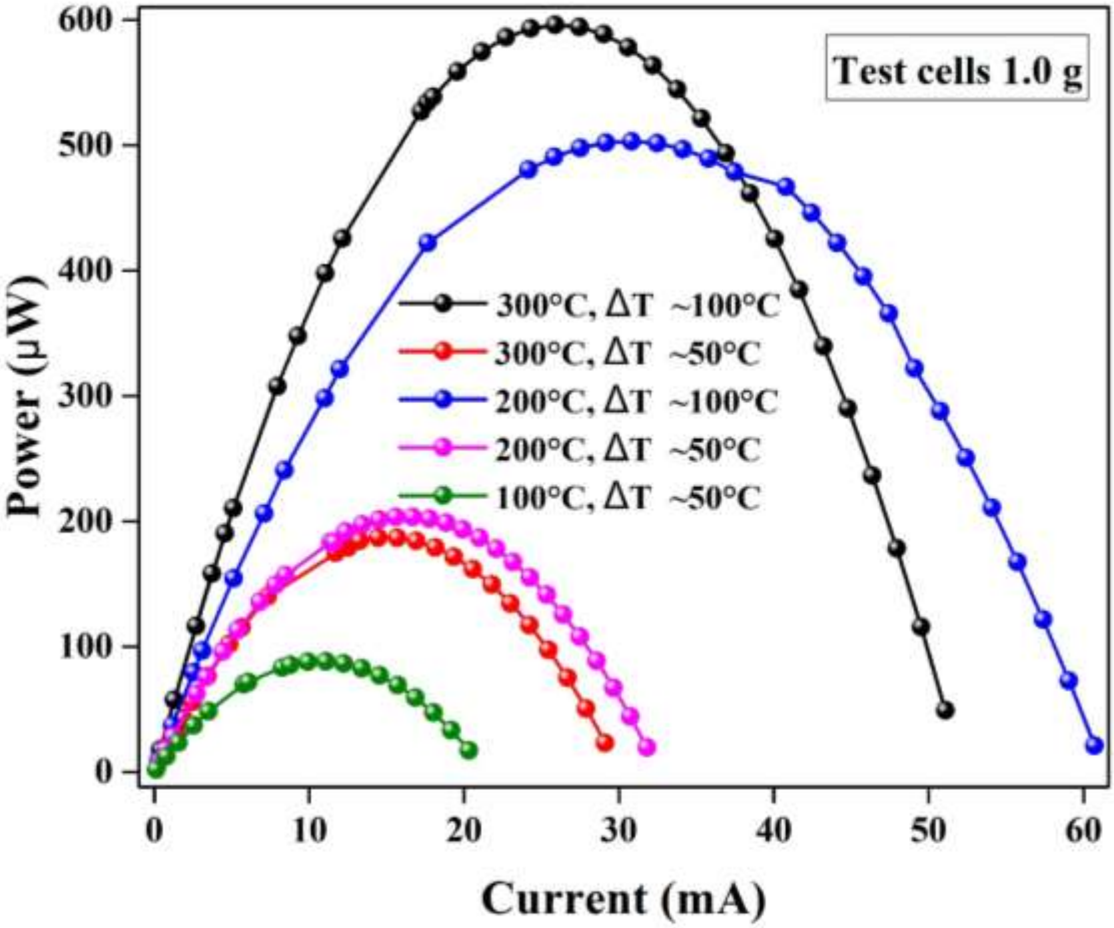

Figure 65 Electrical power output curves of the test cells of monolithic β–Zn_4Sb_3/ZnO TEG module under condition of weight 1.0 g versus different operating T_h and ΔT.

The IV–curves, electrical power output curves and comparative tables of the test cells of monolithic β–Zn_4Sb_3/ZnO TEG modules under conditions of weight 0.2 g, 0.5 g, 2.0 g and 4.0 g are shown in appendix figure and table part.

Table 7 Comparison of maximum electrical power output of test cell of monolithic β–Zn_4Sb_3/ZnO TEG module under condition of weight 1.0 g for different conditions of T_h and ΔT.

Hot–side Temperature	Gradient temperature (ΔT)	Maximum P_{out}
100 °C	50 °C	87 μW
200 °C	50 °C	204 μW
200 °C	100 °C	502 μW
300 °C	50 °C	186 μW
300 °C	100 °C	595 μW

The monolithic multi–stack β–Zn_4Sb_3/ZnO TEG module was measured V_{op} and I_{sc} across its charge terminals. The V_{op} and I_{sc} of the monolithic multi–stack β–Zn_4Sb_3/ZnO TEG module were measured under various operating condition, with a hot side temperature (T_h) of 100 °C and gradient temperature (ΔT) of 50 °C, as well as T_h=200 °C–ΔT=50 °C, T_h=200 °C –ΔT=100 °C, T_h=300 °C –ΔT=50 °C and T_h=300 °C –ΔT=100 °C. The results of V_{op} and I_{sc} of the monolithic multi–stack β–Zn_4Sb_3/ZnO TEG module under all operating conditions are listed in Table 8, as illustrated in Figure 62 and Figure 63.

Table *8* The V_{op} and I_{sc} values for the monolithic multi–stack β–Zn_4Sb_3/ZnO TEG module were found to be 11.6 mV, 36.0 mV, 45.3 mV 47.5 mV, 73.1 mV and 5.11 mA, 14.83 mA, 18.07 mA, 13.53 mA, 18.36 mA, respectively, for T_h=100 °C –ΔT=50 °C, T_h=200 °C –ΔT=50 °C, T_h=200 °C –ΔT=100 °C, T_h=300 °C –ΔT=50 °C and 300°C –ΔT 100 °C, respectively. The results showed an increasing trend in both V_{op} and I_{sc} as T_h and ΔT increased. As depicted in Figure 66, the IV–curves of the multi–stack β–Zn_4Sb_3/ZnO TEG module at operating temperature of T_h=300 °C exhibit a similar steep slope under condition of ΔT=50 °C and ΔT=100 °C, while the intercepts on the current axis differ significantly between these two conditions. Conversely, the IV–curve results at T_h=200 °C appear quite similar to each other, likely due to the effects of low electrical resistivity and the enhanced power factor of the β–Zn_4Sb_3 pellets at an operating temperature of 200 °C, as illustrated in Figure 62 and Figure 63.

Table 8 List of open–circuit voltage (V_{op}) and short circuit current (I_{sc}) versus varying operating condition temperature of the monolithic multi–stack β–Zn_4Sb_3/ZnO TEGs.

Hot–side Temperature	Gradient temperature (ΔT)	Open–circuit voltage (V_{op}) mV	Short circuit current (I_{sc}) mA
100 °C	50 °C	11.6	5.11
200 °C	50 °C	36.0	14.83
200 °C	100 °C	45.3	18.07
300 °C	50 °C	47.5	13.53
300 °C	100 °C	73.1	18.36

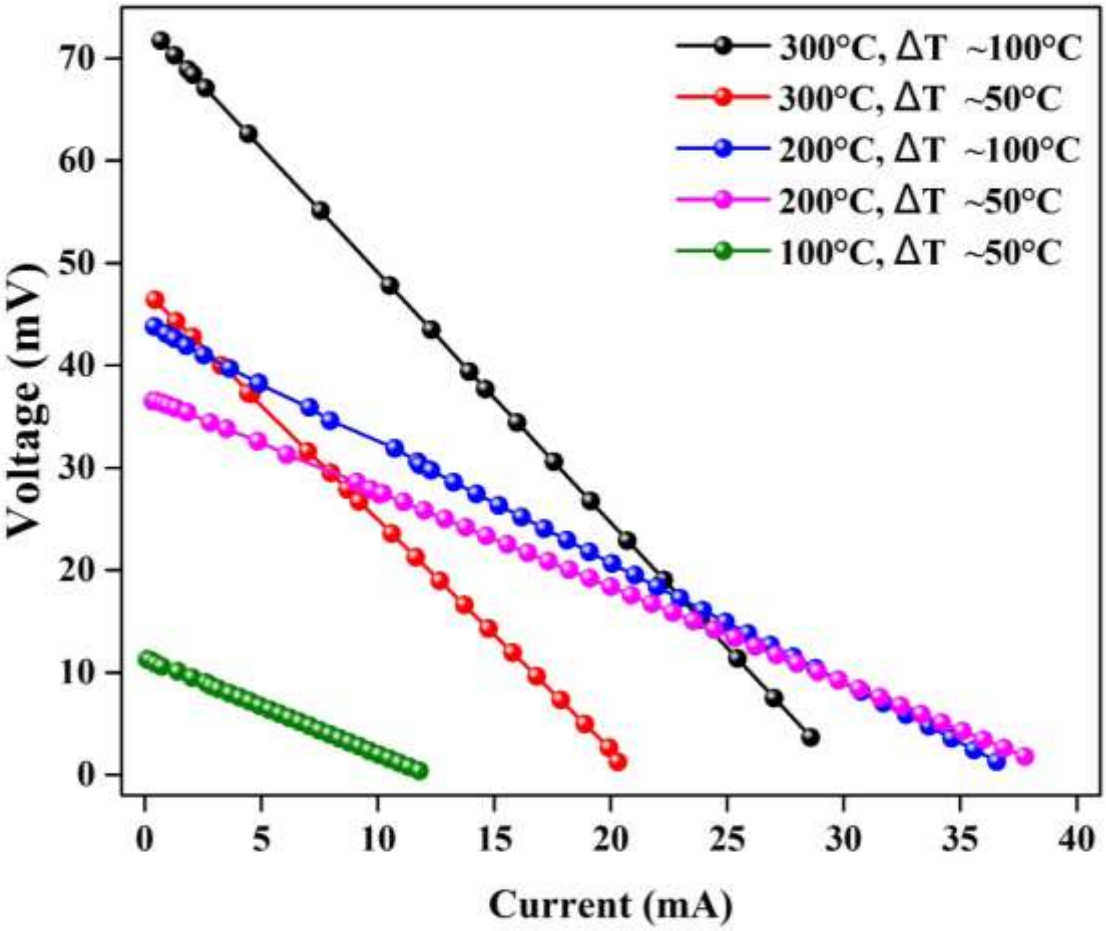

Figure 66 IV characteristics of the monolithic multi–stack β–Zn_4Sb_3/ZnO TEGs versus varying operation hot side temperature and temperature gradients ΔT.

As depicted in Figure 67, the operating condition that produced the highest maximum electrical power output (P_{out}) of 550 μW was T_h=300 °C–ΔT=100 °C, while the lowest P_{out} of 38 μW was observed under the condition of T_h=100 °C–ΔT=50 °C. A comparison of maximum electrical power output (P_{out}) under different operating conditions is provided in Table 9. Although, the maximum electrical power output was achieved under the operating temperature of T_h=300 °C–ΔT=100 °C, the optimal operating temperature for the monolithic β–Zn_4Sb_3/ZnO TEG module is T_h=200 °C. This is because the electrical power output curves at T_h=200 °C of the monolithic β–Zn_4Sb_3/ZnO TEG modules demonstrate remarkably consistent behaviour under both ΔT=50 °C and ΔT=100 °C conditions. The broad and consistent IV–curves and electrical power output curves at T_h=200 °C suggest that the monolithic β–Zn_4Sb_3/ZnO TEG modules is suited for application as an electrical generator that can operate under fluctuation ΔT conditions, specifically within the range of ΔT 50–100 °C at an operating temperature of 200 °C.

Table 9 Results of the maximum electrical power output for different conditions of hot–side temperature and ΔT of the monolithic β–Zn_4Sb_3/ZnO TEGs.

Hot–side Temperature	Gradient temperature (ΔT)	Maximum P_{out}
100 °C	50 °C	38 μW
200 °C	50 °C	370 μW
200 °C	100 °C	418 μW
300 °C	50 °C	250 μW
300 °C	100 °C	550 μW

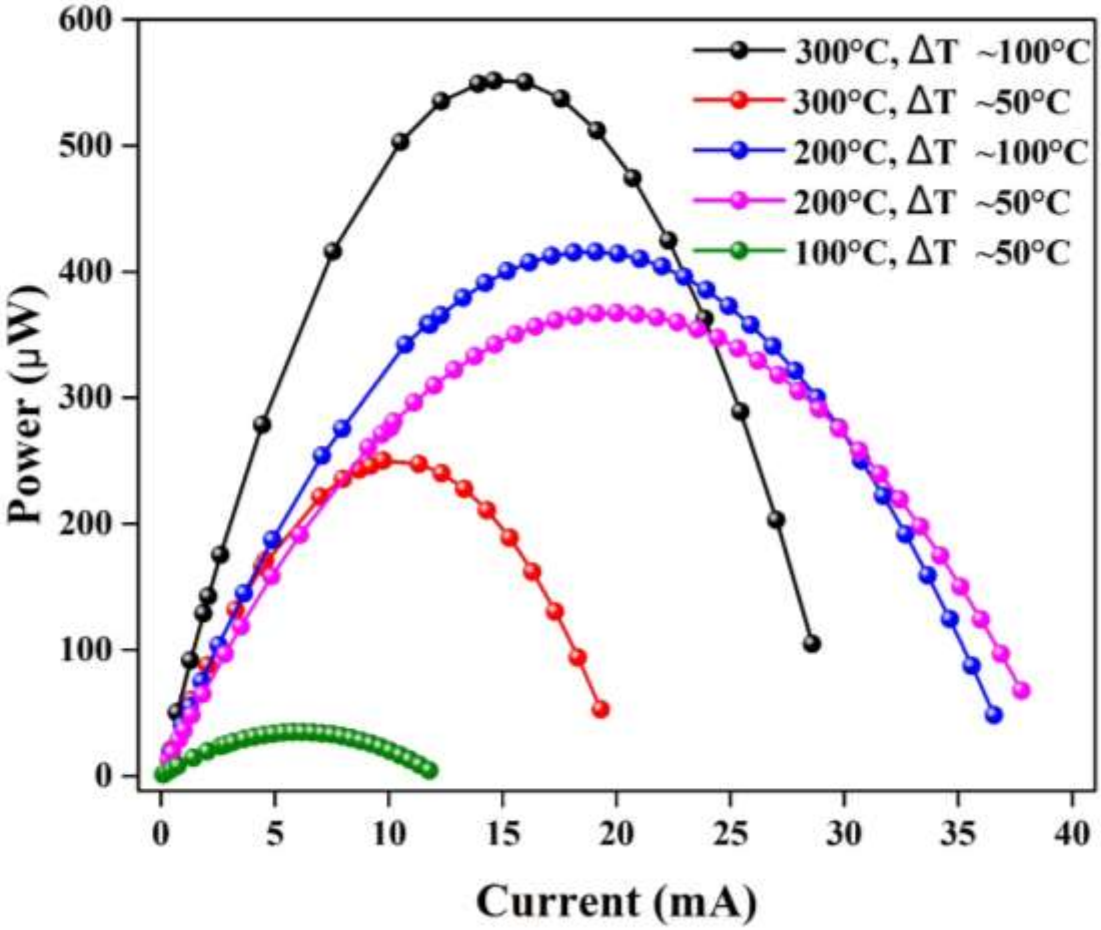

Figure 67 Electrical power output curves of the monolithic multi–stack β–Zn_4Sb_3/ZnO TEGs versus varying operation hot side temperature and temperature gradients ΔT.

Based on the maximum electrical power output of 550 μW, the monolithic β–Zn_4Sb_3/ZnO TEG modules are comparable to other monolithic TEG modules that reported in the literature. A comparison of the maximum electrical power output from this work with of other reports is shown in Table 10.

Table 10 Comparison of the maximum electrical power output versus variant monolithic TEG modules of this work and literature reports.

TE–materials	N–pairs	N–cells	T_h (℃)	ΔT (℃)	P_{out} (μW)	Ref.
Single walled carbon nanotube (SWCNT)	8	16	70	50	7.19	(Hasan *et al.*, 2024)
$Bi_{0.5}Sb_{1.5}Te_3$ & $Ag_2S_{0.2}Se_{0.8}$	3	6	130	50	2,350	(Lai *et al.*, 2022)
$Ni_{0.9}Mo_{0.1}$ & $La_{0.035}Sr_{0.965}TiO_3$	50	100	30	10	100	(Funahashi *et al.*, 2011)
$Cu_{2.075}Se$ & $Ag_2S_{0.55}Se_{0.45}$	1	2	60	30	310	(Ang *et al.*, 2023)
β–Zn_4Sb_3	0	4	300	100	550	this work